Full Hematocrit-Viscosity Curve Identification Using Three-Dataset Krieger-Dougherty Regression

Yang Jun Kang *

Posted Date: 30 March 2026

doi: 10.20944/preprints202603.2339.v1

Keywords: K-D regression model; full hematocrit-viscosity curve; three hematocrit-viscosity datasets; blood viscosity; hematocrit; coflowing streams method; micro hemocytometer; blood separation; microfluidic chip

 doi:10.20944/preprints202603.2339.v1

Article

Full Hematocrit-Viscosity Curve Identification Using Three-Dataset Krieger-Dougherty Regression

Yang Jun Kang

Department of Mechanical Engineering, Chosun University, 10, Chosundae 1-gil, Dong-gu, Gwangju 61452, Republic of Korea; yjkang2011@chosun.ac.kr; Tel.: +82-62-230-7052; Fax: +82-62-230-7055

Abstract

Blood viscosity is strongly dependent on hematocrit, and the hematocrit–viscosity relationship is an important determinant of blood rheology under physiological and pathological conditions. However, obtaining a full hematocrit–viscosity curve requires multiple measurements over a wide hematocrit range. In this study, a simple method is proposed to reconstruct the full hematocrit–viscosity curve using only three-dataset Krieger–Dougherty (K–D) regression as $\mu = \mu_0(1 - \frac{\phi}{\phi_m})^{-\alpha\,\phi_m}$. Based on suspended blood, RBC-rich blood and RBC-depleted blood are prepared after centrifugation. Hematocrit of each blood is measured using a micro hemocytometer. Simultaneously, blood viscosity of each blood is measured using coflowing streams method. The proposed method is evaluated sequentially using reference datasets and hematocrit-viscosity datasets of control blood. According to results, full hematocrit–viscosity curve obtained from selected three datasets is in well agreement with the experimental data and yields lower root-mean-square error than conventional method using all datasets. The exponent of K–D model is strongly influenced by the midpoint dataset whereas μ_0 is mainly affected by suspending medium (dextran solution). In contrast, GA-induced rigidified RBCs do not significantly affect μ_0. In conclusion, the proposed method provides simple, efficient, and reliable approach for estimating the full hematocrit–viscosity curve.

Keywords: K-D regression model; full hematocrit-viscosity curve; three hematocrit-viscosity datasets; blood viscosity; hematocrit; coflowing streams method; micro hemocytometer; blood separation; microfluidic chip

1. Introduction

Blood consists of plasma and cellular components (i.e., red blood cells [RBCs], white blood cells, and platelets)[1]. Blood viscosity is a rheological property that represents resistance of shearing blood flow, which is defined as the ratio of shear stress to shear rate. Clinically, blood viscosity plays a critical role in determining vascular resistance, microcirculatory blood flow, and tissue oxygen supply[2]. An abnormal increase in blood viscosity can hinder blood flow and is closely related to cardiovascular risk[3,4], thrombosis, ischemia, and diabetes[5,6]. Accordingly, blood viscosity is regarded not only as a basic physical parameter of blood circulation, but also as a promising biomarker for evaluating hemorheological abnormalities and the progression of disease.

Blood viscosity is determined by several factors, including, hematocrit[7–15], plasma composition[4,16–21], and RBC rheological properties (i.e., aggregation[22–30], deformability[31–36]). Blood viscosity is governed by shear rate of blood flow (i.e., non-Newtonian fluid). Among the factors influencing blood viscosity, hematocrit is the most important factor affecting blood viscosity. In other words, when blood hematocrit increases, the RBCs become more crowded which makes blood flow more difficult. Consequently, it contributes to increasing blood viscosity[1,2,10,15,37–41].

When blood viscosity is described solely as a function of hematocrit, the corresponding regression model has been progressively refined from a simple linear approximation to a nonlinear asymptotic form. The earliest expression is the Einstein-type relation (i.e., $\frac{\mu}{\mu_0} = 1 + 2.5\,\phi$). Herein, μ,

 doi:10.20944/preprints202603.2339.v1

μ_0, and ϕ denote blood viscosity, plasma viscosity, and hematocrit, respectively. However, this equation is valid only at very low hematocrit (i.e., $\phi < 0.1$) and does not adequately describe whole blood over the physiological hematocrit range. This limitation is later addressed by finite concentration model[42] and more fully resolved by the Krieger–Dougherty (K-D) model[43,44], $\frac{\mu}{\mu_0} = (1 - \frac{\phi}{\phi_m})^{-\alpha \phi_m}$. Herein, a maximum packing factor (ϕ_m) is introduced to represent the steep rise in blood viscosity as hematocrit approaches its upper limit. The exponent ($\alpha \phi_m$) represents both contributions of RBCs to blood viscosity and maximum hematocrit. Accordingly, hematocrit-viscosity relation has been often represented by Krieger-type asymptotic equation[10,45], $\mu = \mu_0(1 - \frac{\phi}{\phi_m})^{-n}$. These forms describe the hematocrit–viscosity relationship over the full hematocrit range.

The major limitation in blood sample preparation is that the hematocrit intended from volumetric mixing is often different from the hematocrit obtained by micro hemocytometer. Considering that hematocrit strongly influences the viscosity of blood suspensions, hematocrit is commonly adjusted by centrifuging whole blood and recombining the concentrated red blood cell fraction with plasma or another suspending medium to obtain nominal target values[10]. However, the packed red blood cell layer obtained after centrifugation is not a pure cell phase because a small amount of plasma is trapped within the packed layer[46,47]. In addition, manual microhematocrit determination introduces reader-dependent variability and other measurement errors which further complicate accurate adjustment of hematocrit[48]. Therefore, when blood samples are prepared by pipetting fixed volumes of concentrated red blood cells and medium, the initially intended hematocrit may differ from the measured value, making post-preparation verification and repeated readjustment essential for obtaining a precise target hematocrit. This is especially important in viscosity experiments, where even small hematocrit deviations can alter the measured hematocrit–viscosity relationship[49]. To minimize hematocrit mismatch during sample preparation, the packed RBC fraction is washed two or three times to reduce residual plasma. The prepared suspension is verified using a standardized hematocrit method and the mixing ratio is then readjusted on the basis of the measured hematocrit rather than the nominal volumetric value[13,14,50]. More recently, hematocrit has been measured by detecting the interface position in a capillary channel [9,51].

In this study, a new method is proposed to identify the full hematocrit–viscosity curve from three hematocrit–viscosity datasets based on the K–D regression model. First, the hematocrit of suspended blood is measured using a centrifuge hemocytometer and is denoted as ϕ_1. Its corresponding viscosity (μ_1) is measured by flowing the sample through a microfluidic chip. Next, centrifugation of the driving syringe separates the blood into RBC-rich and RBC-depleted layers. The hematocrit of the RBC-rich layer is measured as (ϕ_2), while the viscosities of the RBC-rich and RBC-depleted layers are obtained as μ_2 and μ_3, respectively. The hematocrit of the RBC-depleted layer is assumed to be $\phi_3 = 0$. Finally, based on K–D regression model as $\mu = \mu_0(1 - \frac{\phi}{\phi_m})^{-\alpha \phi_m}$, the full hematocrit–viscosity curve is determined from the three hematocrit-viscosity datasets (i.e., ϕ_1 -μ_1, ϕ_2 - μ_2, and ϕ_3 - μ_3).

Compared with the conventional method that requires multiple separately prepared blood samples at different hematocrits, the proposed method offers several advantages. First, it reduces repeated hematocrit adjustment by reconstructing the full hematocrit–viscosity curve from only three datasets. Second, it simplifies the experimental procedure by generating RBC-rich and RBC-depleted fractions directly from a single sample. Third, it decreases blood consumption, preparation time, and inter-sample variability, thereby providing a more efficient and consistent approach for identifying the full hematocrit–viscosity relationship.

2. Materials and Methods

2.1. Measurement of Hematocrit and Blood Viscosity

 doi:10.20944/preprints202603.2339.v1

To obtain full hematocrit-viscosity curve, it was necessary to get hematocrit and blood viscosity, respectively.

As shown in Figure 1A, an experimental setup was composed of a micro hemocytometer for hematocrit (ϕ) and a microfluidic system for blood viscosity (μ). As shown in left-side panel, procedures for measuring hematocrit and blood viscosity were divided into two steps. At the first step, with regard to suspended blood, hematocrit of suspended blood was obtained as ϕ_1. The blood was loaded into a driving syringe. Viscosity of suspended blood was obtained as μ_1 by supplying the blood into a microfluidic chip. The needle (20 G) was removed from the syringe and the syringe end was sealed with a plastic cap. The syringe was placed in a centrifuge (Allegra X-30, Beckman Coulter™, Brea, CA, USA) and rotated at 4000 rpm for 10 min. After centrifugation, suspended blood was separated into RBC-rich layer and RBC-depleted layer (i.e., medium) within the syringe. At the second step, the plastic cap was removed from the syringe and a needle was attached to the syringe. The blood collected in the plastic cap was then used to determine the hematocrit of the RBC-rich blood (ϕ_2). The syringe was mounted on a syringe pump. By operating the syringe pumps, both bloods (i.e., RBC-rich blood and RBC-depleted blood) were delivered sequentially into a microfluidic chip. The corresponding viscosities of RBC-rich blood and RBC-depleted blood was then obtained as μ_2 and μ_3, respectively. For simplicity, the hematocrit of RBC-depleted blood was assumed to be ϕ_3 = 0.

As shown in the middle panel of Figure 1A, a needle was attached to a syringe tip for blood viscosity measurements. The needle was replaced by a plastic cap for separating suspended blood with a centrifuge. Using a micro hemocytometer (VS-18000, Vison Science, Daejeon, South Korea), the corresponding hematocrit values of suspended blood and RBC-rich blood were determined as ϕ_1 and ϕ_2, respectively.

The right-side panel represented blood viscosity measurement using coflowing streams method[52–54]. After test blood and reference fluid were loaded into each syringe, both syringes were positioned in two syringe pumps. Herein, glycerin solution (30%) was selected as reference fluid. As flow rate of each fluid set to Q_b (blood) and Q_r (reference fluid), both fluids were delivered into a microfluidic chip. The microfluidic chip consisted of two inlets, a straight channel (width [w] = 1000 μm, depth = 50 μm), and outlet. To accurately detect blood viscosity, interface between two fluids was relocated near the middle width of channel (β = 0.5) by adjusting flow rate of reference fluid. For simple mathematical representation, both streams in a single channel were mathematically represented using a discrete fluidic circuit model, which consisted of flow-rate (Q_b, Q_r) and fluidic resistance (R_b: fluidic resistance of blood, R_r: fluidic resistance of reference fluid). As each stream had the same pressure in a straight channel, pressure relation between each stream was derived as $P_r \approx P_b$. The P_r and P_b were expressed as $P_r = R_r \times Q_r$ and $P_b = R_b \times Q_b$. Using the same pressure condition of each stream (i.e., $R_r \times Q_r \approx R_b \times Q_b$)[52], viscosity formula of blood (μ_b) was derived as $\mu_b = \mu_r(\frac{\beta}{1-\beta})(\frac{Q_r}{Q_b})$. Herein, the μ_r denoted viscosity of reference fluid.

As shown in Figure 1B, time-lapse blood viscosity was measured through a two-step procedure. Herein, control blood (ϕ_{vol} = 0.5) was prepared by adding normal RBCs (500 μL) into 1× PBS (500 μL). Flow rate of control blood set to Q_b = 5 mL/h. At the first step, hematocrit and viscosity of suspended blood was quantified as ϕ_1 = 0.44 ± 0.01 (n = 4) and μ_1 = 2.02 ± 0.11 cP (n = 124), respectively. At the second step, the corresponding hematocrit-viscosity of RBC-rich blood were obtained as ϕ_2 = 0.97 ± 0.01 (n = 4) and μ_2 = 17.19 ± 3.25 cP (n = 47). The viscosity of RBC-depleted blood was measured as μ_3 = 1.24 ± 0.0 7 cP (n = 117).

 doi:10.20944/preprints202603.2339.v1

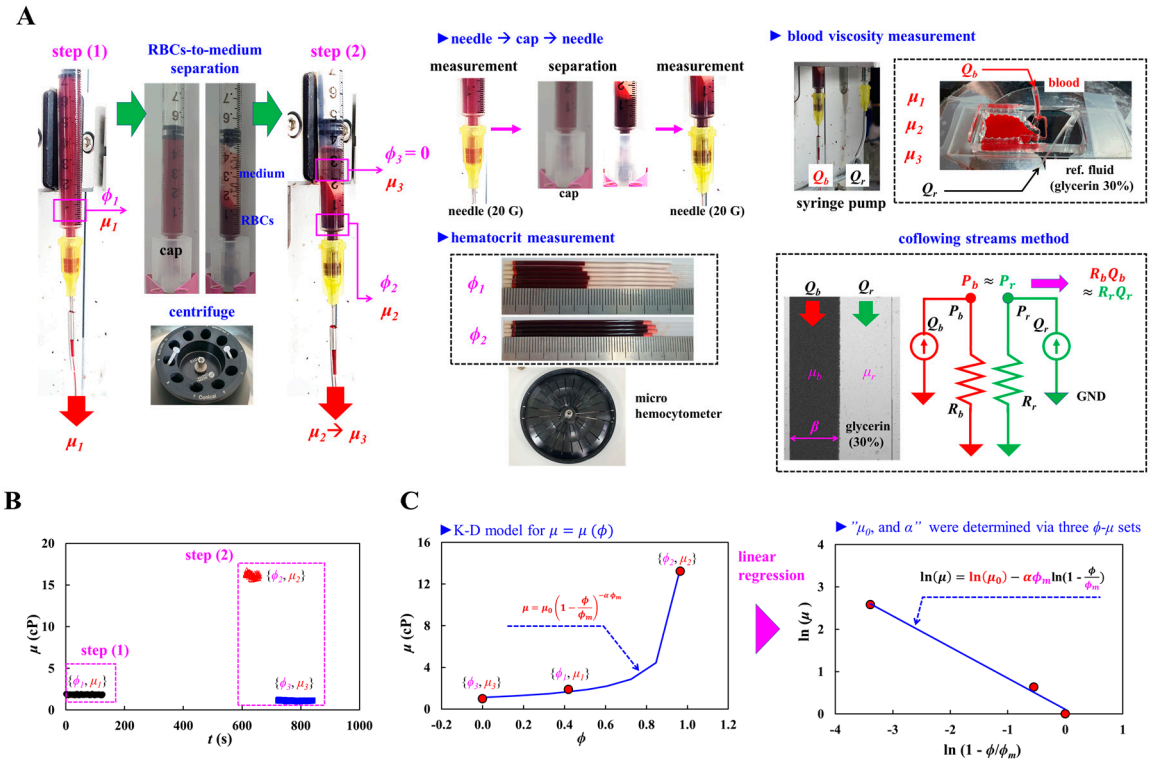

Figure 1. A proposed method for obtaining full hematocrit-viscosity curve. **(A)** Experimental setup, including, micro hemocytometer for hematocrit (ϕ) and a microfluidic system for blood viscosity (μ). The left-side panel showed a two-step measurement of hematocrit and viscosity. The middle-side panel showed replacement of a syringe needle for RBCs-to-medium separation and a micro hemocytometer for hematocrit measurement. The right-side panel showed blood viscosity measurement using coflowing streams method. **(B)** Time-lapse blood viscosity obtained through two steps procedures of measurement. **(C)** Calculation procedure of full hematocrit-viscosity curve using K-D regression model. The left-side panel showed full hematocrit-viscosity curve using K-D model: $\mu = \mu_0(1 - \frac{\phi}{\phi_m})^{-\alpha\phi_m}$. Three hematocrit-viscosity datasets were plotted on hematocrit (ϕ) and viscosity (μ) axes. The right-side panel showed linear regression analysis for obtaining two unknown variables (i.e., μ_0 and α), where the ϕ_m is specified as $\phi_m = 1$. The regression analysis estimated two unknown constants.

To find out regression coefficients of K-D model, as shown in left-side panel of Figure 1C, three hematocrit-viscosity datasets were plotted on hematocrit (ϕ) axis and viscosity (μ) axis. According to the K-D regression model as $\mu = \mu_0(1 - \frac{\phi}{\phi_m})^{-\alpha\phi_m}$, three unknown coefficients should be identified to get full hematocrit-viscosity curve. Herein, if the ϕ_m was assumed as $Q_m = 1$, the remaining two unknown coefficients (i.e., μ_0 and α) could be obtained using linear regression analysis. By taking the natural logarithm of both sides of the K–D model, the K-D regression formula could be rewritten in the linearized form as $\ln(\mu) = \ln(\mu_0) - \alpha\phi_m \times \ln(1 - \phi/\phi_m)$. Horizontal and vertical axes were defined as $\ln(1 - \phi/\phi_m)$ and $\ln(\mu)$. As shown in right-side panel of Figure 1C, three hematocrit-viscosity datasets were then mapped onto horizontal and vertical axes. According to linear regression analysis, two unknown coefficients (μ_0, α) could be estimated accurately. That is, a full hematocrit-viscosity curve could be obtained using three hematocrit-viscosity datasets.

2.2. Blood Sample Preparation

Concentrated erythrocytes were provided by the Gwangju–Chonnam Blood Bank (Gwangju, Republic of Korea) and kept refrigerated until use in the experiment. Based on the established washing method described previously[55], normal RBCs were collected by repeatedly removing supernatant suspension medium and buffy coat.

 doi:10.20944/preprints202603.2339.v1

First, to determine how hematocrit affects blood viscosity, test suspensions were prepared by mixing normal RBCs with 1× PBS to obtain RBC volume fractions (ϕ_{vol}) between 10% and 100%. Second, to further examine the effect of the suspending medium, normal RBCs at a constant volume fraction (ϕ_{vol} = 0.5) were suspended in dextran solutions (C_{dex} = 5 ~ 30 mg/mL). The dextran solutions were made by dissolving dextran powder (Leuconostoc spp., MW 450–650 kDa, Sigma-Aldrich, St. Louis, MO, USA) in 1× PBS. Lastly, the effect of RBC rigidity on blood viscosity was investigated by modulating cell stiffness with glutaraldehyde treatment. Two glutaraldehyde concentrations (C_{GA} = 0.075% and 0.15%) were prepared by diluting a 25% aqueous glutaraldehyde stock solution (Grade II, Sigma-Aldrich, USA) into 1× PBS. Normal RBCs were incubated in each glutaraldehyde solution with stirring for 10 min. Following centrifugation, the fixed RBCs were collected after removal of the supernatant PBS. The final test suspensions were then obtained by resuspending the hardened RBCs into 1× PBS.

2.3. Statistical Analysis

Data analysis was conducted using MINITAB software (Version 22.4, Minitab Inc., State College, PA, USA) and Microsoft Excel (Version 365, Microsoft, Redmond, WA, USA). Under the assumption of normality, all measurements were expressed as mean ($\bar{x}$) ± standard deviation (σ). Number of data was denoted as n. 95% confidence interval (CI) (confidence interval) were determined from $\bar{x} - 1.96\frac{\sigma}{\sqrt{n}}$ to $\bar{x} + 1.96\frac{\sigma}{\sqrt{n}}$. Differences among groups were assessed using one-way ANOVA and statistical significance was accepted at p-value < 0.05. Linear regression analysis was further performed in Microsoft Excel and the resulting slope and intercept were used to calculate two unknown coefficients of K-D regression model.

3. Results and Discussion

3.1. Determination of Maximum Packing Volume Fraction (ϕ_m) in the K-D Regression Model

In this subsection, the maximum packing volume fraction (ϕ_m) in the K–D regression model was determined by carefully evaluating the regression error using the root-mean-square (RMS) value. Two previously reported datasets were used to identify the best-fit curve and the corresponding RMS as a function of ϕ_m.

First, using hematocrit-viscosity data taken from the reference (Pirofsky)[56]), as shown in Figure 2A-i, viscosity (μ) and (ϕ) were plotted along horizontal and vertical axes, respectively. The red-line represented the best-fitted curve determined by linear regression analysis. Figure 2A-ii showed best-fitted curve with respect to ϕ_m = 1.0 and 0.8. Herein, horizontal and vertical axes were defined as ln (1 - ϕ/ϕ_m) and ln (μ), respectively. Hematocrit-viscosity datasets were plotted along the both axes. According to linear regression analysis, the corresponding formular of each ϕ_m was obtained as ln (μ) = -1.3047 ln (1 - ϕ/ϕ_m) + 0.1776 (R^2 = 0.9176) for ϕ_m = 1.0, and ln (μ) = -0.6384 ln (1 - ϕ/ϕ_m) + 0.3933 (R^2 = 0.8801) for ϕ_m = 0.8. That is, the corresponding $\alpha\phi_m$ of each ϕ_m was obtained as $\alpha\phi_m$ = -1.3047 (ϕ_m = 1.0) and $\alpha\phi_m$ = -0.6387 (ϕ_m = 0.8). In addition, the corresponding μ_0 of each ϕ_m was obtained as μ_0 = 1.194 cP (ϕ_m = 1.0) and μ_0 = 1.482 cP (ϕ_m = 1.0). As the coefficient of R^2 was obtained as high value of R^2 = 0.8801 ~ 0.9176, both best-fitted curves represented variations of μ with respect to ϕ sufficiently. As shown in Figure 2A-iii, raw data and best-fitted curves were superimposed along hematocrit (ϕ) and viscosity (μ) axes, respectively, where blue and pink lines represented the best fitted curves obtained by assuming ϕ_m = 0.8 and ϕ_m = 1.0, respectively. The results suggested that the best-fitted curve obtained by assuming ϕ_m = 1.0 was more accurate than that obtained by assuming ϕ_m = 0.8. To assess the effect of ϕ_m on accuracy of regression analysis, multiple data points of ϕ_m were selected between 0.8 to 1.0.

 doi:10.20944/preprints202603.2339.v1

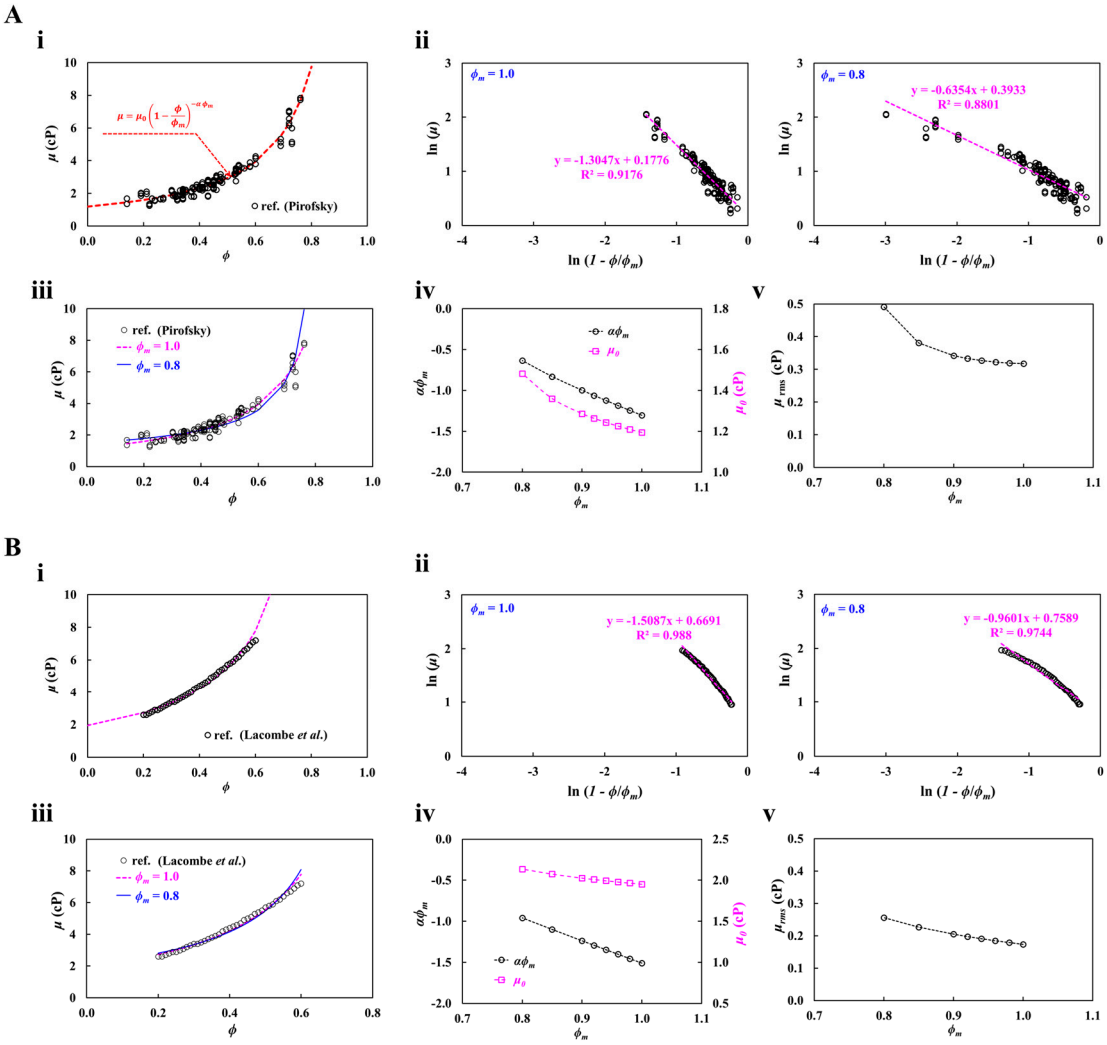

Figure 2. Determination of ϕ_m for K-D regression model using hematocrit-viscosity set taken from two literatures. **(A)** The impact of ϕ_m on accuracy of regression model using hematocrit-viscosity sets taken from the literature (Pirofsky). **(i)** Variations of blood viscosity (μ) with respect to hematocrit (ϕ). The red curve represented best-fitted curve of K-D regression model. **(ii)** Linear curve-fitting procedure with respect to ϕ_m = 1.0 and 0.8. **(iii)** Comparison of a curve-fitting formular with respect to ϕ_m. Blue and pinks line denoted the best fitted curve obtained by assuming ϕ_m = 0.8 and 1.0. **(iv)** Variations of $\alpha\phi_m$ and μ_0 with respect to ϕ_m. **(v)** Variations of root-mean-square value of μ (μ_{rms}) respect to ϕ_m. **(B)** The effect of ϕ_m on K-D model accuracy using hematocrit-viscosity data taken from the literature (Lacombe *et al.*). **(i)** Variations of μ with respect to ϕ. (ii) Linear curve-fitting procedure with respect to ϕ_m = 1.0 and 0.8. According to linear regression analysis, the corresponding formular of each ϕ_m was obtained as ln (μ) = -1.5087 ln (1 - ϕ/ϕ_m) + 0.6691 (R^2 = 0.988) for ϕ_m = 1.0, and ln (μ) = -0.9601 ln (1 - ϕ/ϕ_m) + 0.7589 (R^2 = 0.8801) for ϕ_m = 0.8. **(iii)** Comparison of the best fitted curve with respect to ϕ_m = 0.8 and 1.0. **(iv)** Variations of $\alpha\phi_m$ and μ_0 with respect to ϕ_m. **(v)** Variations of μ_{rms} respect to ϕ_m.

As shown Figure 2A-iv, linear regression analysis yielded the changes in $\alpha\phi_m$ and μ_0 as a function of ϕ_m. According to the results, as ϕ_m increased from 0.8 to 1.0, $\alpha\phi_m$ and μ_0 tended to decrease gradually, confirming that the ϕ_m had a strong impact on determination on both coefficients. In addition, to evaluate accuracy of regression analysis, root-mean-square (RMS) value of μ (i.e., μ_{rms}) was calculated with respect to ϕ_m. Herein, the μ_{rms} represented the average deviation between measured and predicted values (i.e., $\mu_{rms} = \sqrt{\frac{1}{n}\sum_{i=1}^{i=n}(\mu_i - \hat{\mu}_i)^2}$, μ_i: measured viscosity, and $\hat{\mu}_i$: predicted viscosity). As shown in Figure 2A-v, the variations of μ_{rms} were plotted as a function of ϕ_m.

 doi:10.20944/preprints202603.2339.v1

The results indicated that higher value of ϕ_m led to a substantial decrease in μ_{rms}. Accordingly, the most accurate curve-fitting was obtained when ϕ_m was set to 1.0.

Second, hematocrit-viscosity data taken from the literature (Lacombe *et al.*)[57] was additionally used to validate the contribution of ϕ_m to accuracy of regression analysis. Figure 2B-i depicted all hematocrit-viscosity datasets and a best-fitted curve of K-D regression model. As shown in Figure 2B-ii, according to linear regression analysis, best fitted curve was obtained by assuming $\phi_m = 1.0$ and $\phi_m = 0.8$. As a result, the corresponding formular of each ϕ_m was obtained as $\ln(\mu) = -1.5087 \ln(1 - \phi/\phi_m) + 0.6691$ ($R^2 = 0.988$) for $\phi_m = 1.0$, and $\ln(\mu) = -0.9601 \ln(1 - \phi/\phi_m) + 0.7589$ ($R^2 = 0.8801$) for $\phi_m = 0.8$. That is, the corresponding $\alpha\phi_m$ of each ϕ_m was estimated as $\alpha\phi_m = -1.5087$ ($\phi_m = 1.0$) and $\alpha\phi_m = -0.9601$ ($\phi_m = 0.8$). Additionally, the corresponding μ_0 of each ϕ_m was estimated as $\mu_0 = 1.952$ cP ($\phi_m = 1.0$) and $\mu_0 = 2.136$ cP ($\phi_m = 0.8$). To validate accuracy of a best-fitted curve, as shown in Figure 2B-iii, experimental datasets and both regression curves were superimposed on hematocrit (ϕ) and viscosity (μ) axes. The results indicated that both best-fitted curves were well matched with experimental datasets. To investigate contribution of ϕ_m to coefficients (i.e., $\alpha\phi_m$ and μ_0), multiple values of ϕ_m were selected between 0.8 and 1.0. As shown in Figure 2B-iv, variations of $\alpha\phi_m$ and μ_0 were obtained with respect to ϕ_m. The results indicated that the ϕ_m contributed to decreasing both coefficients substantially. Specifically, the ϕ_m had a strong influence on determination of $\alpha\phi_m$ and μ_0. As shown in Figure 2B-v, to validate accuracy of best-fitted curve, variations of μ_{rms} were obtained respect to ϕ_m. According to results, the μ_{rms} tended to decrease gradually at higher value of ϕ_m. Thus, it is necessary to set $\phi_m = 1.0$ for getting more accurate best-fitting curve.

From the curve-fitting analysis of two kinds of previous hematocrit-viscosity datasets, the maximum packing volume fraction (ϕ_m) in the K–D regression model had a strong influenced on determination on $\alpha\phi_m$ and μ_0. Additionally, the root-mean-square value of best-fitted curve was minimized at higher value of $\phi_m = 1.0$. Based on the simulation study, the study adopted $\phi_m = 1.0$ for getting a best-fitted curve of hematocrit-viscosity datasets.

From the curve-fitting analysis of two previously reported hematocrit–viscosity datasets, the maximum packing volume fraction (ϕ_m) in the K–D regression model was found to strongly affect the determination of $\alpha\phi_m$ and μ_0. In addition, the root-mean-square error of the fitted curve was minimized when a higher value of $\phi_m = 1.0$ was used. Based on this simulation analysis, $\phi_m = 1.0$ was adopted to obtain the best-fitted hematocrit–viscosity curve.

3.2. Hematocrit-Viscosity Measurement Datasets of Control Blood

In this subsection, with regard to control blood, full hematocrit-viscosity datasets were obtained at higher shear rates (i.e., $\dot{\gamma} > 10^3$ s^{-1}). Herein, the control blood was prepared by adding normal RBCs into 1× PBS.

First, to determine the appropriate blood flow rate of the syringe pump (Q_b), blood viscosity (μ) was measured over flow rate ranging from $Q_b = 1$ mL/h to $Q_b = 5$ mL/h. Following the previously reported coflowing-streams method[52], the reference-fluid flow rate (Q_r) was adjusted so that the interface was positioned near the center of the channel width. RBC volume fraction in the blood set to $\phi_{vol} = 0.5$. As shown in Figure 3A-i, six number of control blood ($S_n = 6$) was set to probe variation of hematocrit (ϕ). The inset exhibited capillary tubes used for measuring hematocrit. Dashed lines represented 95% CI (i.e., $0.431 < \phi < 0.445$). Next, blood viscosity of control blood was obtained with respect to Q_b. To relocate interface near center of channel width, with respect to Q_b, the corresponding flow-rate of reference fluid was set to $Q_r = 1$ mL/h (Q_b =1 mL/h), $Q_r = 2$ mL/h ($Q_b = 2$ mL/h), $Q_r = 2.5$ mL/h ($Q_b = 3$ mL/h), $Q_r = 4$ mL/h ($Q_b = 4$ mL/h), $Q_r = 4.2$ mL/h ($Q_b = 5$ mL/h), and $Q_r = 5$ mL/h ($Q_b = 6$ mL/h). The corresponding interface of both flow-rate conditions was measured as $\beta = 0.460 \pm 0.004$ ($Q_b = 1$ mL/h, $Q_r = 1$ mL/h), $\beta = 0.442 \pm 0.002$ ($Q_b = 2$ mL/h, $Q_r = 2$ mL/h), $\beta = 0.477 \pm 0.003$ ($Q_b = 3$ mL/h, $Q_r = 2.5$ mL/h), $\beta = 0.462 \pm 0.003$ ($Q_b = 4$ mL/h, $Q_r = 4$ mL/h), $\beta = 0.468 \pm 0.005$ ($Q_b = 5$ mL/h, $Q_r = 4.2$ mL/h), and $\beta = 0.464 \pm 0.005$ ($Q_b = 6$ mL/h, $Q_r = 5$ mL/h). As shown in left-side panel of **Figure 3A-ii**, blood viscosity of control blood was obtained with respect to Q_b. The corresponding viscosity of each flow-rate was obtained as $\mu = 2.29 \pm 0.03$ cP ($n = 164$, $Q_b = 1$ mL/h), $\mu = 2.12 \pm 0.02$ cP ($n = 189$, $Q_b = 2$

 doi:10.20944/preprints202603.2339.v1

mL/h), μ = 2.04 ± 0.03 cP (n = 194, Q_b = 3 mL/h), μ = 2.02 ± 0.03 cP (n = 108, Q_b = 4 mL/h), μ = 1.98 ± 0.04 cP (n = 181, Q_b = 5 mL/h), and μ = 1.94 ± 0.04 cP (n = 74, Q_b = 6 mL/h). Based on the shear rate formula[52] (i.e., $\dot{\gamma} = \frac{6\,Q_b}{\beta\, w\, h^2}$), the corresponding shear rate of each blood-flow rate was estimated as $\dot{\gamma}$ =1451.5 s^{-1} (Q_b = 1 mL/h), $\dot{\gamma}$ = 3020 s^{-1} (Q_b = 2 mL/h), $\dot{\gamma}$ = 4194.1 s^{-1} (Q_b = 3 mL/h), $\dot{\gamma}$ = 5773.2 s^{-1} (Q_b = 4 mL/h), $\dot{\gamma}$ = 7130.1 s^{-1} (Q_b = 5 mL/h), and $\dot{\gamma}$ = 8617.7 s^{-1} (Q_b = 6 mL/h). The right-side panel of Figure 3A-ii exhibited variations of blood viscosity with respect to Q_b. Blood viscosity decreased substantially over Q_b = 1 ~ 3 mL/h, whereas only a slight decrease was observed over Q_b = 3 ~ 6 mL/h. Based on these results, Q_b = 1 and 5 mL/h were selected for measuring blood viscosity at higher shear rates.

Second, hematocrit-viscosity datasets were obtained at Q_b = 1 and 5 mL/h. As shown in Figure 3B-i, hematocrit-viscosity datasets were obtained at Q_b = 1 mL/h. The left-side panel showed relationship between ϕ and ϕ_{vol}. Herein, the ϕ_{vol} of control blood was adjusted to ϕ_{vol} = 0.1 ~ 1.0. The corresponding hematocrit of each blood was obtained with micro hemocytometer. The dashed-line exhibited 95% CI. Inset showed representative images used to determine RBC-volume fraction (ϕ) in a micro capillary tube following centrifugation. According to linear regression analysis, best fitted curve was obtained as ϕ = 0.908 ϕ_{vol} (R^2 = 0.9986). The middle-side panel exhibited variations of μ with respect to ϕ_{vol}. Number of viscosity data at each ϕ_{vol} was ranged from n = 316 to n = 2234. The right-side panel showed variations of μ with respect to ϕ. The corresponding viscosity of each hematocrit was obtained as μ = 1.14 ± 0.03 cP (ϕ = 0.08 ± 0.002), μ = 1.37 ± 0.03 cP (ϕ = 0.17 ± 0.006), μ = 1.60 ± 0.04 cP (ϕ = 0.24 ± 0.006), μ = 1.92 ± 0.05 cP (ϕ = 0.33 ± 0.004), μ = 2.26 ± 0.05 cP (ϕ = 0.42 ± 0.007), μ = 2.66 ± 0.08 cP (ϕ = 0.52 ± 0.005), μ = 3.38 ± 0.08 cP (ϕ = 0.64 ± 0.005), μ = 4.10 ± 0.12 cP (ϕ = 0.71 ± 0.006), μ = 5.99 ± 0.18 cP (ϕ = 0.82 ± 0.003), and μ = 11.56 ± 0.83 cP (ϕ = 0.93 ± 0.011). On the other hand, as shown in Figure 3B-ii, hematocrit-viscosity datasets were obtained at Q_b = 5 mL/h. The left-side panel showed relationship between ϕ and ϕ_{vol}. According to linear regression analysis, a best fitted curve was obtained as ϕ = 0.903 ϕ_{vol} (R^2 = 0.993). The middle-side panel exhibited variations of μ with respect to ϕ_{vol}. Number of viscosity data at each ϕ_{vol} was ranged from n = 52 to n = 260. The right-side panel showed variations of μ with respect to ϕ. The corresponding viscosity of each hematocrit was obtained as μ = 1.24 ± 0.02 cP (ϕ = 0.16 ± 0.006), μ = 1.43 ± 0.02 cP (ϕ = 0.16 ± 0.007), μ = 1.63 ± 0.02 cP (ϕ = 0.32 ± 0.004), μ = 1.89 ± 0.03 cP (ϕ = 0.42 ± 0.006), μ = 2.24 ± 0.03 cP (ϕ = 0.51 ± 0.008), μ = 2.80 ± 0.04 cP (ϕ = 0.61 ± 0.006), μ = 3.89 ± 0.08 cP (ϕ = 0.72 ± 0.007), μ = 6.34 ± 0.16 cP (ϕ = 0.85 ± 0.009), and μ = 13.23 ± 0.26 cP (ϕ = 0.97 ± 0.011).

Experimental measurements provided two hematocrit–viscosity datasets at Q_b = 1 and 5 mL/h, which were used to validate the accuracy of the proposed method for reconstructing the full hematocrit–viscosity curve based on the K–D regression model.

 doi:10.20944/preprints202603.2339.v1

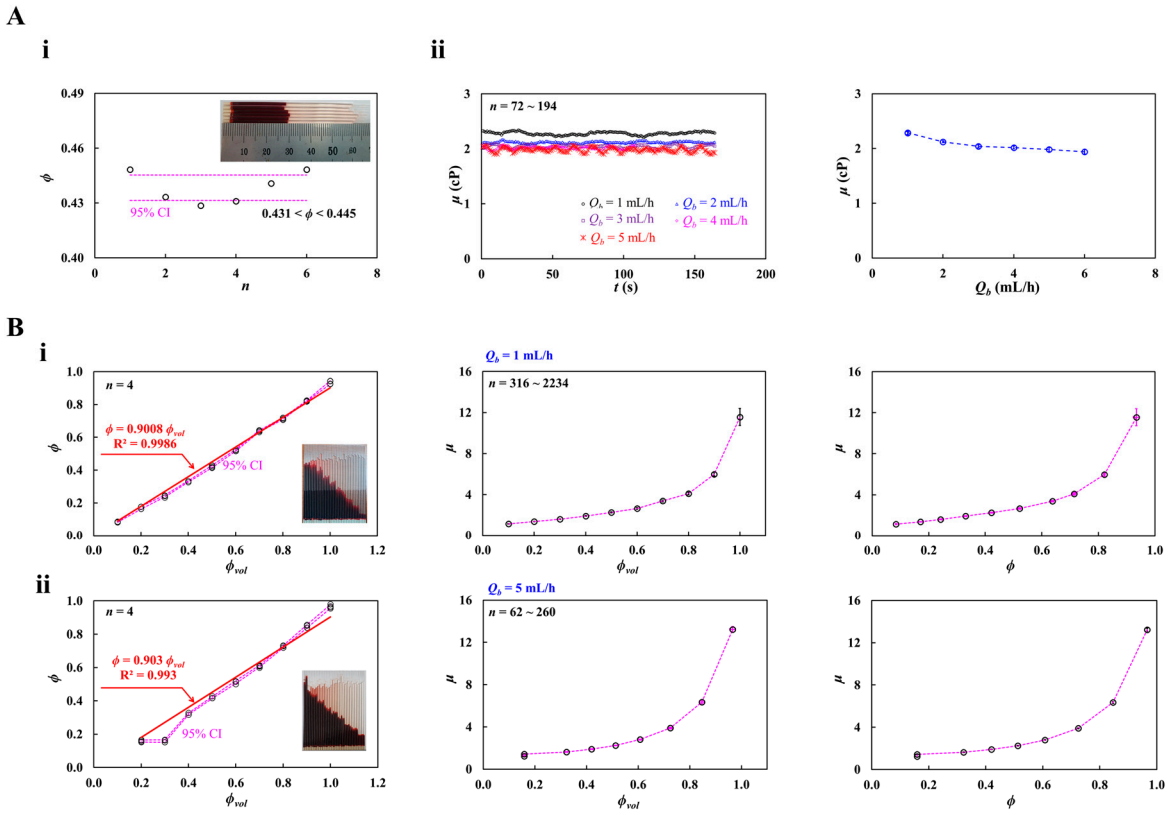

Figure 3. Experimental measurement of hematocrit-viscosity datasets of control blood at high shear rate. The control blood was prepared by adding normal RBCs into 1× PBS. **(A)** Determination of blood flow rate (Q_b). Herein, RBC volume fraction in the blood set to ϕ_{vol} = 0.5. **(i)** Variations of hematocrit (ϕ) for six number of control blood (S_n = 6). Dashed line denoted 95% confidential intervals (i.e., 0.431 < ϕ < 0.445). **(ii)** Variations of μ with respect to blood-flow rate (Q_b). The left-side panel showed time-lapse viscosity with respect to Q_b ranging from Q_b = 1 mL/h to Q_b = 6 mL/h. The right-side panel showed variations of μ with respect to Q_b. **(B)** Measurement of hematocrit-viscosity datasets at Q_b = 1 and 5 mL/h. **(i)** Measurement of ϕ - μ obtained at Q_b =1 mL/h. The left-side panel showed relationship between ϕ and ϕ_{vol}. The dashed-line exhibited 95% CI. The mid-side panel exhibited variations of μ with respect to ϕ_{vol}. The right-side panel showed variations of μ with respect to ϕ. **(ii)** Measurement of ϕ - μ obtained at Q_b =5 mL/h. The left-side panel showed relationship between ϕ and ϕ_{vol}. The dashed-line exhibited 95% CI. The mid-side panel exhibited variations of μ with respect to ϕ_{vol}. The right-side panel showed variations of μ with respect to ϕ.

3.3. Quantitative Evaluation of Proposed Method Using Hematocrit-Viscosity Datasets of Control Blood

In this subsection, as shown in Figure 3B, the proposed method for getting full hematocrit-viscosity curve was validated using experimental data. Herein, with respect to each hematocrit, blood viscosity was obtained at Q_b = 1 and 5 mL/h.

First, validation of proposed method was conducted using eleven hematocrit-viscosity datasets, where blood viscosity was measured at the flow rate of Q_b = 1 mL/h ($\dot{\gamma}$ = 1451.5 s^{-1}). Figure 4A represented complete hematocrit-viscosity curve identification using eleven ϕ - μ datasets. Herein, the ϕ_m was set to ϕ_m = 1.0. As shown in left-side panel, hematocrit-viscosity datasets were mapped on ln (1 - ϕ/ϕ_m) and ln (μ) axes. According to linear regression analysis, best fitted curve was obtained as ln (μ) = -0.8873 ln (1 - ϕ/ϕ_m) + 0.2085 (R^2 = 0.9711). From the curve-fitting formula, $\alpha\phi_m$ and μ_0 were obtained as $\alpha\phi_m$ = -0.8873 and μ_0 = 1.238 cP, respectively. As shown in right-side panel, best fitted curve of $\mu = 1.238\,(1-\phi)^{-0.8873}$ was superimposed on all hematocrit-viscosity datasets. The results showed that the best-fitted curve was in good agreement with the experimental datasets, except at the highest hematocrit value of ϕ = 0.934. The root-mean-square error was estimated as μ_{rms} = 0.714 cP. Using all experimental datasets as shown in Figure 4A, full hematocrit-viscosity curve was

 doi:10.20944/preprints202603.2339.v1

identified using three ϕ - μ datasets. Herein, both boundary datasets (i.e., ϕ_2 = 0.934: μ_2 = 11.56 cP, and ϕ_3 = 0: μ_3 = 1 cP) were fixed during hematocrit-viscosity curve identification. Middle point dataset (ϕ_1 = 0.08 ~ 0.82) was only selected from the remaining nine datasets. As show in Figure 4B-i, full hematocrit-viscosity curve was calculated using midpoint dataset (i.e., ϕ_1 = 0.33, μ_1 = 1.917 cP). According to linear regression analysis, best-fitted curve was obtained as ln (μ) = -0.856 ln (1 - ϕ) + 0.1415 (R^2 = 0.985). α and μ_0 were estimated as α = -0.856 and μ_0 = 1.152 cP, respectively. Complete hematocrit-viscosity curve was then identified as $\mu = 1.152\ (1-\phi)^{-0.856}$. Additionally, root-mean-square error was estimated as μ_{rms} = 0.475 cP. Similarly, as shown in Figure 4B-ii, full hematocrit-viscosity curve was estimated using midpoint dataset (i.e., ϕ_1 = 0.422, μ_1 = 2.264 cP). According to linear regression analysis, best-fitted curve was obtained as ln (μ) = -0.8564 ln (1 - ϕ) + 0.1547 (R^2 = 0.9797). α and μ_0 were estimated as α = -0.8564 and μ_0 = 1.167 cP, respectively. Complete hematocrit-viscosity curve was then identified as $\mu = 1.167\ (1-\phi)^{-0.8564}$. The root-mean-square error was estimated as μ_{rms} = 0.459 cP. As shown in Figure 4B-iii, full hematocrit-viscosity curve was calculated using midpoint dataset (i.e., ϕ_1 = 0.521, μ_1 = 2.657 cP). According to linear regression analysis, best-fitted curve was obtained as ln (μ) = -0.8658 ln (1 - ϕ) + 0.1433 (R^2 = 0.9796). α and μ_0 were estimated as α = -8658 and μ_0 = 1.154 cP, respectively. Full hematocrit-viscosity curve was then identified as $\mu = 1.154\ (1-\phi)^{-0.8658}$. The root-mean-square error was estimated as μ_{rms} = 0.475 cP. Figure 4C exhibited quantitative comparison of full hematocrit-viscosity curve obtained by all datasets and three datasets. Left-side panel exhibited variations of α with respect to selected midpoint dataset (ϕ_1). The dashed line represented α = 0.8873 obtained by all hematocrit-viscosity datasets. The value of α was strongly affected by the selected midpoint dataset. Mid-side panel showed variations of μ_0 with respect to selected midpoint dataset (ϕ_1). The dashed line represented μ_0 = 1.238 cP obtained by all hematocrit-viscosity datasets. Considering that the blood viscosity at ϕ = 0 was measured as μ = 1.028 cP, the μ_0 estimated from all hematocrit–viscosity datasets was overestimated by approximately 20.4%. Moreover, the μ_0 values obtained from the three selected datasets were lower than those derived from the full dataset, with minimum values at low and high hematocrit and maximum value near ϕ = 0.33 – 0.52. Right-side panels depicted variations of μ_{rms} with respect to midpoint dataset (ϕ_1). The dashed line represented μ_{rms} = 0.714 cP obtained by all hematocrit-viscosity datasets. The proposed method using three selected datasets yielded a lower root-mean-square error than the conventional method using all datasets. In particular, when ϕ was selected between 0.33 and 0.52, the root-mean-square error was estimated as μ_{rms} = 0.475 ~ 0.495 cP. These results indicated that the full hematocrit–viscosity curve obtained from the three selected datasets was more accurate and remained in good agreement with the overall hematocrit–viscosity datasets.

 doi:10.20944/preprints202603.2339.v1

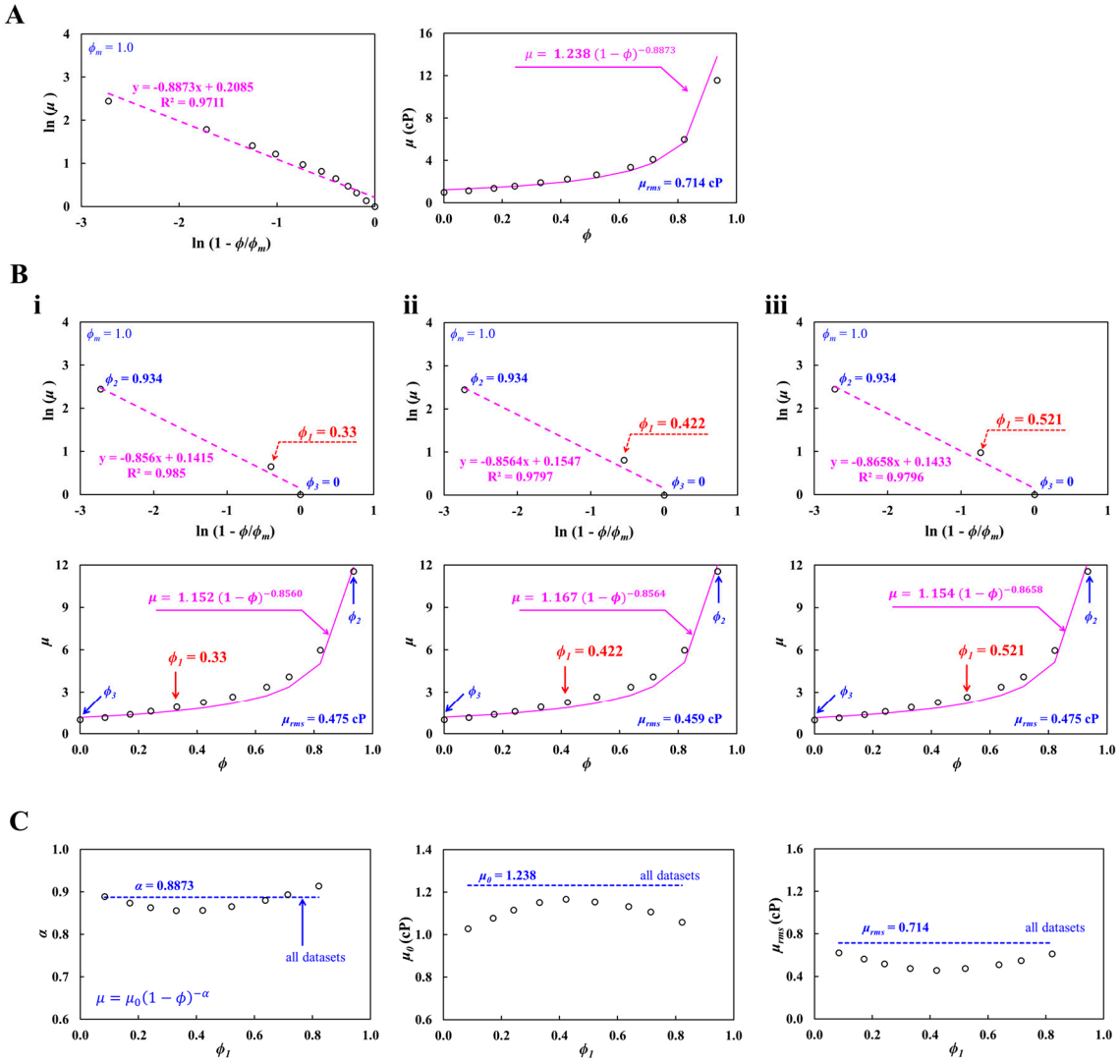

Figure 4. Validation of proposed method using eleven hematocrit-viscosity sets, where blood viscosity was measured at the flow rate of Q_b = 1 mL/h. **(A)** Complete hematocrit-viscosity curve identification using eleven ϕ - μ datasets. As shown in left-side panel, hematocrit-viscosity datasets were mapped on ln (1-ϕ/ϕ_m) and ln (μ) axes. Right-side panel showed all hematocrit-viscosity datasets and their best fitted curve of $\mu = 1.238\ (1-\phi)^{-0.8873}$. **(B)** Regression formula using three ϕ - μ datasets. Herein, both boundary datasets (i.e., ϕ_2 = 0.934: μ_2 = 11.56 cP, and ϕ_3 = 0: μ_3 = 1 cP) were fixed to get complete hematocrit-viscosity curve. Middle point dataset (ϕ_1) was selected from the remaining nine datasets. **(i)** Full hematocrit-viscosity curve using midpoint dataset (i.e., ϕ_1 = 0.33, μ_1 = 1.917 cP). Complete hematocrit-viscosity curve and root-mean-square error were obtained as $\mu = 1.152\ (1-\phi)^{-0.8560}$ and μ_{rms} = 0.475 cP. **(ii)** Full hematocrit-viscosity curve using midpoint dataset (i.e., ϕ_1 = 0.422, μ_1 = 2.264 cP). Complete hematocrit-viscosity curve and root-mean-square error were estimated as $\mu = 1.167\ (1-\phi)^{-0.8564}$ and μ_{rms} = 0.459 cP. **(iii)** Full hematocrit-viscosity curve using midpoint dataset (i.e., ϕ_1 = 0.521, μ_1 = 2.657 cP). Full hematocrit-viscosity curve and root-mean-square error were calculated as $\mu = 1.154\ (1-\phi)^{-0.8658}$ and μ_{rms} = 0.475 cP. **(C)** Quantitative comparison of full hematocrit-viscosity curve obtained from all datasets (i.e., conventional method) and selected three datasets (i.e., proposed method). The dashed line represented α = 0.8873, μ_0 = 1.238 cP, and μ_{rms} = 0.714 cP obtained from all hematocrit-viscosity datasets. Left-side panel exhibited variations of α with respect to selected midpoint dataset (ϕ_1). Mid-side panel showed variations of μ_0 with respect to selected midpoint dataset (ϕ_1). Right-side panels depicted variations of μ_{rms} with respect to midpoint dataset (ϕ_1). .

Second, full hematocrit-viscosity curve was estimated using ten hematocrit-viscosity datasets, where blood viscosity was measured at Q_b = 5 mL/h ($\dot{\gamma}$ = 7130.1 s^{-1}). Figure 5A depicted full

 doi:10.20944/preprints202603.2339.v1

hematocrit-viscosity curve obtained from ten ϕ - μ datasets. Herein, ϕ_m was set to $\phi_m = 1.0$. As shown in left-side panel, linear regression analysis gave best fitted curved as ln (μ) = -0.7637 ln (1 - ϕ) + 0.2082 (R^2 = 0.9672). α and μ_0 were then obtained as α = 0.7637 and μ_0 = 1.2318 cP. As shown in in right-side panel, full hematocrit-viscosity curve of $\mu = 1.2315\,(1-\phi)^{-0.7637}$ was superimposed on all hematocrit-viscosity datasets. The results showed that the best-fitted curve was in satisfactory agreement with the experimental datasets. Root-mean-square error was estimated as μ_{rms} = 1.083 cP.

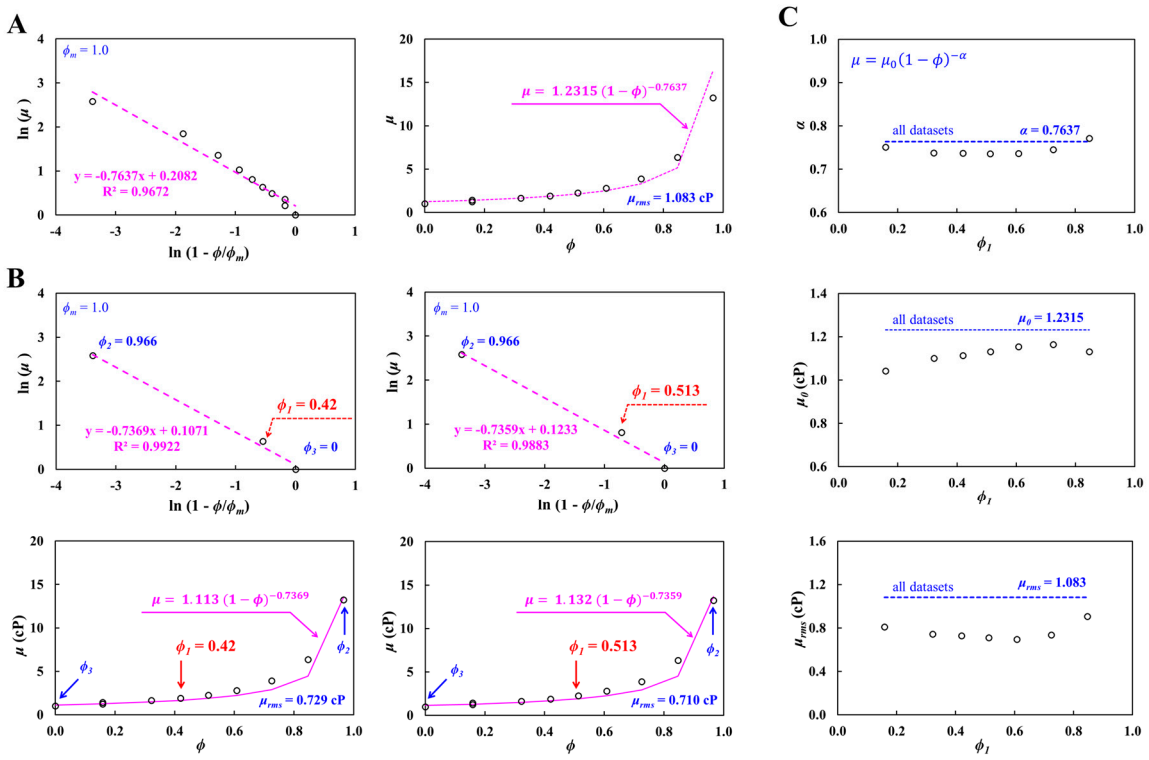

Figure 5. Validation of proposed method using ten hematocrit-viscosity datasets, where blood viscosity was measured at Q_b = 5 mL/h. **(A)** Full hematocrit-viscosity curve identification using ten ϕ - μ datasets. As shown in left-side panel, linear regression analysis gave best fitted curved as ln (μ) = -0.7637 ln (1 - ϕ) + 0.2082 (R^2 = 0.9672). As depicted in right-side panel, full hematocrit-viscosity curve of $\mu = 1.2315(1-\phi)^{-0.7637}$was superimposed on all hematocrit-viscosity datasets. Root-mean-square error was estimated as μ_{rms} = 1.083 cP. **(B)** Full hematocrit-viscosity curve identification using three ϕ - μ datasets. Herein, both boundary datasets (i.e., ϕ_2 = 0.966: μ_2 = 13.23 cP, and ϕ_3 = 0: μ_3 = 1 cP) were fixed during the identification of the complete hematocrit–viscosity curve. First, with regard to midpoint dataset (i.e., ϕ_1 = 0.42, μ_1 = 1.889 cP), Full hematocrit-viscosity curve and root-mean-square error were obtained as $\mu = 1.113\,(1-\phi)^{-0.7369}$ and μ_{rms} = 0.729 cP. Second, with regard to midpoint dataset (i.e., ϕ_1 = 0.513, μ_1 = 2.245 cP), Full hematocrit-viscosity curve and root-mean-square error were obtained as $\mu = 1.132\,(1-\phi)^{-0.7359}$ and μ_{rms} = 0.71 cP. **(C)** Quantitative comparison of full hematocrit-viscosity curve obtained by all datasets and three datasets. The dashed line represented α = 0.7637, μ_0 = 1.2315 cP, and μ_{rms} = 1.083 cP obtained from all hematocrit-viscosity datasets. Upper-side panel exhibited variations of α with respect to midpoint dataset (ϕ_1). Mid-side panel showed variations of μ_0 with respect to midpoint dataset (ϕ_1). Lower-side panels depicted variations of μ_{rms} with respect to midpoint dataset (ϕ_1). .

As shown in Figure 5B, full hematocrit-viscosity curve identification was obtained from selected three ϕ - μ datasets. In the identification of the complete hematocrit–viscosity curve, both boundary datasets (i.e., ϕ_2 = 0.966: μ_2 = 13.23 cP, and ϕ_3 = 0: μ_3 = 1 cP) were fixed. Midpoint dataset (ϕ_1) was selected from the remaining eight datasets. As shown in left-side panel, with regard to midpoint dataset (i.e., ϕ_1 = 0.42, μ_1 = 1.889 cP), best-fitted curve was obtained as ln (μ) = -0.7369 ln (1 - ϕ) + 0.1071 (R^2 = 0.9922). α and μ_0 were then obtained as α = 0.7369 and μ_0 = 1.113 cP. Full hematocrit-viscosity curve and root-mean-square error were obtained as $\mu = 1.113\,(1-\phi)^{-0.7369}$ and μ_{rms} = 0.729 cP. As

 doi:10.20944/preprints202603.2339.v1

shown in right-side panel, with regard to midpoint dataset (i.e., ϕ_1 = 0.513, μ_1 = 2.245 cP), best-fitted curve was obtained as ln (μ) = -0.7359 ln (1 - ϕ) + 0.1233 (R^2 = 0.9883). Full hematocrit-viscosity curve and root-mean-square error were obtained as $\mu = 1.132\ (1-\phi)^{-0.7359}$ and μ_{rms} = 0.71 cP. As shown in Figure 5C, coefficients of K-D regression model (α, μ_0) and root-mean-square error (μ_{rms}) were plotted as a function of selected midpoint dataset (ϕ_1). The dashed line represented α = 0.7637, μ_0 = 1.2315 cP, and μ_{rms} = 1.083 cP obtained from all hematocrit-viscosity datasets. Upper-side panel exhibited variations of α with respect to midpoint dataset (ϕ_1). The results revealed a strong dependence of α on ϕ_1. Mid-side panel showed variations of μ_0 with respect to midpoint dataset (ϕ_1). The μ_0 obtained from selected three datasets was lower than that derived from the full dataset. Lower-side panels depicted variations of μ_{rms} with respect to midpoint dataset (ϕ_1). According to the results, the μ_{rms} obtained from selected three datasets was much lower than that derived from the full dataset.

From the identification of full hematocrit-viscosity curve, the exponent of K-D model was found to depend strongly on the midpoint dataset (ϕ_1, μ_1). The μ_0 and μ_{rms} values obtained from selected three datasets were substantially lower than those obtained from all hematocrit-viscosity datasets. Therefore, full hematocrit-viscosity curve reconstructed from the selected three datasets could be considered more accurate when compared with full hematocrit-viscosity curve obtained from all hematocrit-viscosity curve.

3.4. Contribution of Suspending Medium to Full Hematocrit-Viscosity Curve

In this subsection, to evaluate contribution of suspending medium to full hematocrit-viscosity curve[45,58], specific concentration of dextran solution (C_{dex} = 0 ~ 30 mg/mL) was prepared as blood medium. Herein, C_{dex} = 0 denoted 1× PBS. Test blood (ϕ_{vol} = 0.5) was then prepared by adding normal RBCs into specific concentration of dextran solution. Blood viscosity was obtained at the flow rate of 5 mL/h.

As shown in Figure 6A, three hematocrit-viscosity datasets were presented for C_{dex} = 0, 15, and 30 mg/mL. The left, middle, and right panels showed the datasets for C_{dex} = 0, 15, and 30 mg/mL, respectively. The number of test blood samples was set to S_n = 3 ~ 4.

Using hematocrit-viscosity datasets with respect to test blood (C_{dex}), linear regression analysis was conduced to find out coefficients of K-D regression model (i.e., α, and μ_0). Best-fitted curve and full hematocrit-viscosity curve were then represented with respect to C_{dex} = 0, 15, and 30 mg/mL. Figure 6B-i represented linear regression and full hematocrit-viscosity curve for test blood (C_{dex} = 0). Linear regression analysis gave best fitted curve as ln (μ) = -0.7037 ln (1 - ϕ) + 0.1606 (R^2 = 0.9993). α and μ_0 of K-D model were identified as α = 0.7037 and μ_0 = 1.174 cP. Full hematocrit-viscosity curve was then obtained as $\mu = 1.174\ (1-\phi)^{-0.7037}$. Figure 6B-ii depicted linear regression and full hematocrit-viscosity curve for blood (C_{dex} = 15 mg/mL). Linear regression analysis gave best fitted curve as ln (μ) = -0.7121 ln (1 - ϕ) + 0.7368 (R^2 = 0.9993). Full hematocrit-viscosity curve was then obtained as $\mu = 2.089\ (1-\phi)^{-0.7121}$. Figure 6B-iii showed linear regression and full hematocrit-viscosity curve for blood (C_{dex} = 30 mg/mL). Linear regression analysis provided best fitted curve as ln (μ) = -0.6241 ln (1 - ϕ) + 1.3091(R^2 = 0.9967). Full hematocrit-viscosity curve was then obtained as $\mu = 3.703\ (1-\phi)^{-0.6241}$.

 doi:10.20944/preprints202603.2339.v1

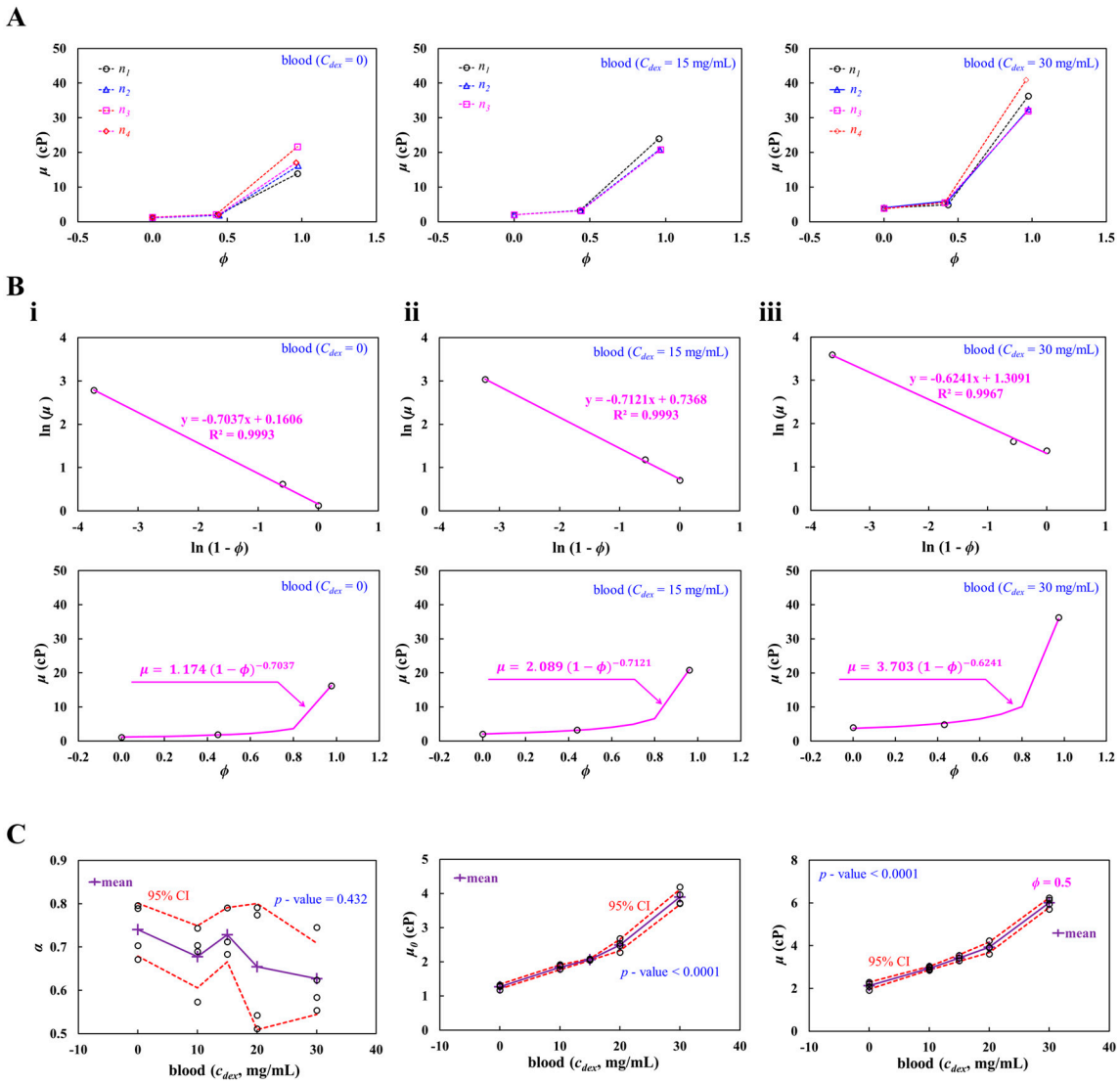

Figure 6. Contribution of blood medium to full hematocrit-viscosity curve. Herein, test blood was prepared by adding normal RBCs into specific concentration of dextran solution (C_{dex} = 5 ~ 30 mg/mL). Blood viscosity was obtained at the flow rate of 5 mL/h. **(A)** Three hematocrit-viscosity datasets with respect to C_{dex} = 0, 15, and 30 mg/mL. **(B)** Full hematocrit-viscosity curve identification with respect to C_{dex}. **(i)** Linear regression and full hematocrit-viscosity curve for blood (C_{dex} = 0). **(ii)** Linear regression and full hematocrit-viscosity curve for blood (C_{dex} = 15 mg/mL). **(iii)** Linear regression and full hematocrit-viscosity curve for blood (C_{dex} = 30 mg/mL). **(C)** Contribution of dextran solution to α, μ_0, and μ (ϕ = 0.5). Left-side panel showed variations of α with respect to C_{dex}. The red-dashed line represented 95% CI. Mid-side panel depicted variations of μ_0 with respect to C_{dex}. Right-side panel showed variations of μ (ϕ = 0.5) with respect to C_{dex}.

Based on full hematocrit-viscosity curve obtained from three datasets, as shown in Figure 6C, variations of α, μ_0, and μ (ϕ = 0.5) was represented at a function of C_{dex}. Left-side panel showed variations of α with respect to C_{dex}. The red-dashed line represented 95% CI. The α tended to decrease slightly over C_{dex}. From statistical test (i.e., ANOVA-test, p-value = 0.432), the dextran solution did not contribute to decreasing α significantly. Mid-side panel depicted variations of μ_0 with respect to C_{dex}. According to statistical test (i.e., ANOVA-test, p - value < 0.001), dextran solution had a strong impact on μ_0. Considering previous studies[59–61], it was confirmed that dextran solution contributed to increasing μ_0 significantly. Based on full hematocrit-viscosity curve, blood viscosity was estimated at ϕ = 0: μ (ϕ = 0.5). Right-side panel showed variations of μ (ϕ = 0.5) with respect to C_{dex}. The results indicated that blood viscosity was increased significantly at higher concentrations of dextran

 doi:10.20944/preprints202603.2339.v1

solution. Statistical test (i.e., ANOVA-test, p - value < 0.001) confirmed that dextran solution had a strong impact on viscosity of suspended blood (ϕ = 0.5).

The experimental results showed that the exponent (α) of the K–D model did not differ significantly with respect to dextran concentration, whereas μ_0 increased markedly as dextran concentration increased. These findings suggested that suspending medium had a strong effect on μ_0 of K–D regression model.

3.5. Contribution of Rigidified RBCs to Full Hematocrit-Viscosity Curve

At the last subsection, to evaluate contribution of rigidified RBCs to full hematocrit-viscosity curve[62–64], normal RBCs were rigidified by incubating them into GA solution. 1× PBS was selected as blood medium. Test blood (ϕ_{vol} = 0.5) was then prepared by adding GA-induced rigidified RBCs into 1× PBS. Blood viscosity of test blood was measured at the flow rate of 5 mL/h.

As shown in Figure 7A, with respect to GA-concentration (C_{GA} = 0, 0.075%, and 0.15 %), three hematocrit-viscosity datasets were plotted on $\phi - \mu$ axes. Herein, the C_{GA} denoted 1× PBS. The number of test blood was set to S_n = 3 ~ 4. Hematocrit of test blood (ϕ) varied substantially, even though RBC volume fraction was fixed at 0.5. Based on three hematocrit-viscosity datasets, linear regression analysis was conducted to get full hematocrit-viscosity curve with respect to C_{GA}.

Figure 7B-i showed linear regression analysis and full hematocrit-viscosity curve for test blood (C_{GA} = 0). According to linear regression analysis, best-fitted curve was obtained as ln (μ) = -0.7409 ln (1 – ϕ) + 0.4477 (R^2 = 0.9934). Two coefficients (α, μ_0) of K-D model were obtained as α = 0.7409 and μ_0 = 1.564 cP. Full hematocrit-viscosity curve was then obtained as $\boldsymbol{\mu = 1.565\,(1 - \phi)^{-0.7409}}$. Figure 7B-ii depicted linear regression analysis and full hematocrit-viscosity curve for blood (C_{GA} = 0.075%). Linear regression analysis gave best fitted curve as ln (μ) = -0.7595 ln (1 – ϕ) + 0.3815 (R^2 = 0.989). Two coefficients (α, μ_0) of K-D model were obtained as α = 0.7595 and μ_0 = 1.464 cP. Full hematocrit-viscosity curve was then obtained as $\mu = 1.464\,(1 - \phi)^{-0.7595}$. Figure 7B-iii exhibited linear regression analysis and full hematocrit-viscosity curve for blood (C_{GA} = 0.15%). Linear regression analysis gave best fitted curve as ln (μ) = -0.6499 ln (1 – ϕ) + 0.4159 (R^2 = 0.9812). Full hematocrit-viscosity curve was then obtained as $\boldsymbol{\mu = 1.516\,(1 - \phi)^{-0.6499}}$.

 doi:10.20944/preprints202603.2339.v1

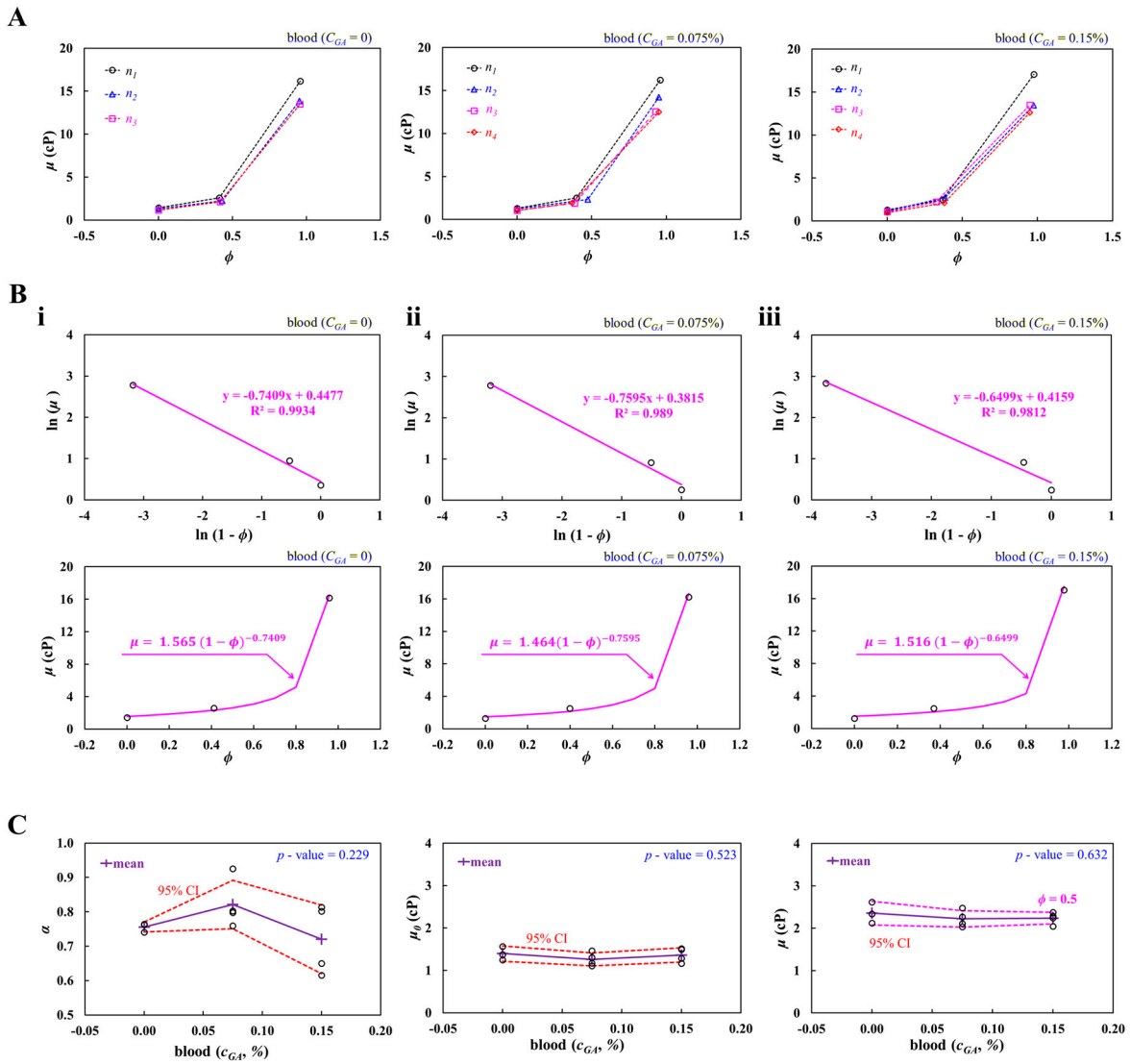

Figure 7. Contribution of RBC deformability to full hematocrit-viscosity curve. Herein, test blood was prepared by adding GA-induced rigidified RBCs into 1× PBS. Blood viscosity of test blood was measured at the flow rate of 5 mL/h. **(A)** Three hematocrit-viscosity datasets with respect to GA-concentration (C_{GA} = 0, 0.075%, and 0.15 %). **(B)** Full hematocrit-viscosity curve identification with respect to C_{GA}. **(i)** Linear regression and full hematocrit-viscosity curve for blood (C_{GA} = 0). **(ii)** Linear regression and full hematocrit-viscosity curve for blood (C_{GA} = 0.075%). **(iii)** Linear regression and full hematocrit-viscosity curve for blood (C_{GA} = 0.15%). **(C)** Contribution of GA-treated hardened RBCs to α, μ_0, and μ (ϕ = 0.5). Left-side panel showed variations of α with respect to C_{GA}. Mid-side panel depicted variations of μ_0 with respect to C_{GA}. Right-side panel showed variations of μ (ϕ = 0.5) with respect to C_{GA}.

As shown in Figure 7C, variation of α, μ_0, and μ (ϕ = 0.5) were plotted as a function of C_{GA}. Left-side panel showed variations of α with respect to C_{GA}. The red-dashed line represented 95% CI. From statistical test (i.e., ANOVA-test, p-value = 0.229), the GA-treated hardened RBCs did not contribute to decreasing α significantly. Specifically, the α decreased slightly between C_{GA} = 0.075% and C_{GA} = 0.15%. Mid-side panel depicted variations of μ_0 with respect to C_{GA}. According to statistical test (i.e., ANOVA-test, p - value = 0.523), the GA-induced rigidified RBCs did not affect μ_0 significantly. Furthermore, because 1× PBS was used as the suspending medium for the test blood, μ_0 was confirmed to be independent of the GA-solution concentration. Right-side panel showed variations of μ (ϕ = 0.5) with respect to C_{GA}. The blood viscosity did not show a substantial difference with respect to C_{GA}. Statistical test (i.e., ANOVA-test, p - value = 0.632) confirmed that the rigidified RBCs did not have a strong impact on viscosity of suspended blood (ϕ = 0.5). According to the previous

 doi:10.20944/preprints202603.2339.v1

study[60], blood viscosity (ϕ_{vol} = 0.3) did not show a substantial difference for up to C_{GA} = 0.1%. Thus, it was inferred that the present results showed consistent trends with respect to C_{GA}.

From the experimental results, rigidified RBCs did not have a strong impact on coefficients of K-D regression model. Blood viscosity (ϕ = 0.5) remained constant for up to C_{GA} = 0.15%.

4. Conclusions

This study demonstrated the feasibility of reconstructing the full hematocrit–viscosity curve from only three selected datasets using the K–D regression model. The results suggested that full hematocrit–viscosity curve obtained from selected three datasets was in well agreement with the experimental data and yielded lower fitting error than the conventional method using all datasets. The exponent of the K–D model was strongly influenced by the midpoint hematocrit whereas μ_0 is mainly affected by suspending medium. In contrast, GA-induced rigidified RBCs did not significantly affect μ_0. In conclusion, the proposed method provided simple, efficient, and reliable approach for estimating the full hematocrit–viscosity curve. As a limitation of this study, the proposed method was validated only under limited experimental conditions, including, specific flow rates, dextran concentrations, and GA concentrations. Because the experiments were conducted using in vitro test blood prepared with dextran solution or GA-induced rigidified RBCs in 1× PBS, the results may not fully represent the rheological behavior of native whole blood under physiological conditions. Therefore, further studies with larger sample sizes and broader experimental conditions will be needed to validate the robustness and practical applicability of the proposed method.

Funding: Please add: This work was supported by the Basic Science Research Program through the NRF funded by the Ministry of Education (NRF-2021R1I1A3040338).

Institutional Review Board Statement: This study was performed in accordance with the Declaration of Helsinki and was approved by the Ethics Committee of Chosun University (reference code: 2-1041055-AB-N-01-2021-80).

Informed Consent Statement: Not applicable.

Data Availability Statement: The original contributions presented in this study are included in the article material. Further inquiries can be directed to the corresponding author.

Acknowledgments: During the preparation of this manuscript, the author used ChatGPT (Ver. 5.4) for the purposes of generating text. The author has reviewed and edited the output and takes full responsibility for the content of this publication.

Conflicts of Interest: The author declares no conflicts of interest.

References

1. Baskurt, O.K.; Meiselman, H.J. Blood rheology and hemodynamics. Semin. Thromb. Hemost. **2003,** 29, 435-450.
2. Sitina, M.; Stark, H.; Schuster, S. Optimal hematocrit theory: a review. J. Appl. Physiol. **2024,** 137, 494-509.
3. Subendran, S.; Wang, Y.C.; Lu, Y.H.; Chen, C.Y. The evaluation of zebrafish cardiovascular and behavioral functions through microfluidics. Sci Rep **2021,** 11, 13801.
4. Peters, S.A.; Woodward, M.; Rumley, A.; Tunstall-Pedoe, H.D.; Lowe, G.D. Plasma and blood viscosity in the prediction of cardiovascular disease and mortality in the Scottish Heart Health Extended Cohort Study. Eur. J. Prev. Cardiol. **2017,** 24, 161-167.
5. Deng, Y.; Papageorgiou, D.P.; Li, X.; Perakakis, N.; Mantzoros, C.S.; Dao, M.; Karniadakis, G.E. Quantifying fibrinogen-dependent aggregation of red blood cells in type 2 diabetes mellitus. Biophys. J. **2020,** 119, 900-912.
6. Cho, Y.I.; Mooney, M.P.; Cho, D.J. Hemrheological disorders in diabetes mellitus. J. diabetes Sci. Technol. **2008,** 2, 1130-1138.

 doi:10.20944/preprints202603.2339.v1

7. Waltz, X.; Hardy-Dessources, M.D.; Lemonne, N.; Mougenel, D.; Lalanne-Mistrih, M.L.; Lamarre, Y.; Tarer, V.; Tressieres, B.; Etienne-Julan, M.; Hue, O.; Connes, P. Is there a relationship between the hematocrit-to-viscosity ratio and microvascular oxygenation in brain and muscle? Clin Hemorheol Microcirc **2015,** 59, 37-43.
8. Mehri, R.; Mavriplis, C.; Fenech, M. Red blood cell aggregates and their effect on non-Newtonian blood viscosity at low hematocrit in a two-fluid low shear rate microfluidic system. PLoS One **2018,** 13, e0199911.
9. Kim, B.J.; Lee, Y.S.; Zhbanov, A.; Yang, S. A physiometer for simultaneous measurement of whole blood viscosity and its determinants: hematocrit and red blood cell deformability. Analyst **2019,** 144, 3144-3157.
10. Trejo-Soto, C.; Hernandez-Machado, A. Normalization of blood viscosity according to the hematocrit and the shear rate. Micromachines (Basel) **2022,** 13, 357.
11. Li, G.; Ye, T.; Yang, B.; Wang, S.; Li, X. Temporal-spatial heterogeneity of hematocrit in microvascular networks. Physics of Fluids **2023,** 35, 021906.
12. Riera-Llobet, C.; Méndez-Mora, L.; Cabello-Fusarés, M.; Hernández-Machado, A. Altered blood rheology in multiwidth microchannels: Hematocrit and tonicity variation. Physics of Fluids **2023,** 35, 082017.
13. Zhao, H.; Han, H.; Lin, Q.; Huang, L.; Su, X.; Fang, Y.; Zhang, Y.; Su, E.; Chen, Z.; Li, S.; Deng, Y.; He, N. A new hematocrit measurement method using a chemiluminescence biosensor and its application in a chemiluminescence immunoassay platform for myocardial markers detection with whole blood samples. Biosensors (Basel) **2023,** 13, 3.
14. Zucchini, L.; Ajcevic, M.; Coda Zabetta, C.D.; Greco, C.; Fernetti, C.; Moretto, C.; Pennini, S.; Accardo, A. Characterization of a novel approach for neonatal hematocrit screening based on penetration velocity in lateral flow test strip. Sensors (Basel) **2023,** 23, 2813.
15. Lee, C.A.; Paeng, D.G. Spatiotemporal blood viscosity by local hematocrit under pulsatile flow: Whole blood experiments and computational analysis. Comput Biol Med **2025,** 198, 111253.
16. Illibauer, J.; Clodi-Seitz, T.; Zoufaly, A.; Aberle, J.H.; Weninger, W.J.; Foedinger, M.; Elsayad, K. Diagnostic potential of blood plasma longitudinal viscosity measured using Brillouin light scattering. Proc Natl Acad Sci U S A **2024,** 121, e2323016121.
17. Chen, W.; Xia, M.; Zhu, W.; Xu, Z.; Cai, B.; Shen, H. A bio-fabricated tesla valves and ultrasound waves-powered blood plasma viscometer. Front Bioeng Biotechnol **2024,** 12, 1394373.
18. Bakhtiaridoost, S.; Musuroi, C.; Volmer, M.; Florescu, M. Optoelectronic microfluidic device for point-of-care blood plasma viscosity measurement. Lab Chip **2024,** 24, 3305-3314.
19. Gautam, N.; Ram, R.; Bishnoi, V.; Sarkar, A. A low-cost and disposable capillary-based paper sensor for measuring blood-plasma viscosity using a smartphone app. Microfluidics and Nanofluidics **2023,** 27, 41.
20. Kang, H.; Jang, I.; Song, S.; Bae, S.C. Development of a paper-based viscometer for blood plasma using colorimetric analysis. Anal Chem **2019,** 91, 4868-4875.
21. Lee, K.; Kinnunen, M.; Khokhlova, M.D.; Lyubin, E.V.; Priezzhev, A.V.; Meglinski, I.; Fedyanin, A.A. Optical tweezers study of red blood cell aggregation and disaggregation in plasma and protein solutions. J Biomed Opt **2016,** 21, 35001.
22. Kang, Y.J. Assessment of continuous flow-dependent red cell aggregation using a microfluidic chip. Applied Sciences **2025,** 15, 11481.
23. Charansonney, O.L.; Meseguer, E.; Goube, P.; Vicaut, E. Erythrocyte aggregation kinetics for studying the vascular phase of inflammation in patients with suspected acute coronary syndrome or acute stroke. Sci Rep **2025,** 15, 38049.
24. Alexandrova-Watanabe, A.; Abadjieva, E.; Ivanova, M.; Gartcheva, L.; Langari, A.; Guenova, M.; Tiankov, T.; Nikolova, E.V.; Krumova, S.; Todinova, S. Quantitative assessment of red blood cell disaggregation in chronic lymphocytic leukemia via software image flow analysis. Fluids **2025,** 10, 167.
25. Lee, C.A.; Farooqi, H.M.U.; Paeng, D.G. Axial shear rate: A hemorheological factor for erythrocyte aggregation under Womersley flow in an elastic vessel based on numerical simulation. Comput Biol Med **2023,** 157, 106767.
26. Weber-Fishkin, S.; Seidner, H.S.; Gunter, G.; Frame, M.D. Erythrocyte aggregation in sudden flow arrest is linked to hyperthermia, hypoxemia, and band 3 availability. J. Thromb. Haemost. **2022,** 20, 2284-2292.

 doi:10.20944/preprints202603.2339.v1

27. Maung Ye, S.S.; Kim, S. A mechanistic model of cross-bridge migration in RBC aggregation and disaggregation. Front Bioeng Biotechnol **2022,** 10, 1049878.
28. Charansonney, O.L.; Morel, P.; Dufaux, J.; Vicaut, E. Description and validation of a new, simple, easy-to handle, point-of-care technique for measuring erythrocyte aggregation kinetics. Sci Rep **2022,** 12, 14798.
29. Lee, C.A.; Paeng, D.G. Numerical simulation of spatiotemporal red blood cell aggregation under sinusoidal pulsatile flow. Sci Rep **2021,** 11, 9977.
30. Namgung, B.; Lee, T.; Tan, J.K.S.; Poh, D.K.H.; Park, S.; Chng, K.Z.; Agrawal, R.; Park, S.Y.; Leo, H.L.; Kim, S. Vibration motor-integrated low-cost, miniaturized system for rapid quantification of red blood cell aggregation. Lab Chip **2020,** 20, 3930-3937.
31. You, J.; Park, C.-A.; Kim, A.-K.; Jeon, H.R.; Kim, D.-I.; Shin, S. Ultrasensitive microfluidic detection of red blood cell deformability: Age-related decline in deformability. Physics of Fluids **2025,** 37,
32. Liu, W.; Xie, L.; Yang, J.; Gong, X.; Sun, D.; Zhang, C. A microfluidic device for detecting the deformability of red blood cells. Biosensors (Basel) **2025,** 15, 758.
33. Kajitani, K.; Ohtani, T.; Higuchi, R.; Chimura, M.; Sera, F.; Tsai, C.D.; Ueda, Y.; Nishimura, J.I.; Sakata, Y. An on-chip deformability checker demonstrates that the severity of iron deficiency is associated with increased deformability of red blood cells. Sci Rep **2025,** 15, 19994.
34. Williams, D.C.; Wood, D.K. High-throughput quantification of red blood cell deformability and oxygen saturation to probe mechanisms of sickle cell disease. Proc Natl Acad Sci U S A **2023,** 120, e2313755120.
35. Kang, Y.J.; Serhrouchni, S.; Makhro, A.; Bogdanova, A.; Lee, S.S. Simple assessment of red blood cell deformability using blood pressure in capillary channels for effective detection of subpopulations in red blood cells. ACS Omega **2022,** 7, 38576-38588.
36. Matrai, A.A.; Varga, G.; Tanczos, B.; Barath, B.; Varga, A.; Horvath, L.; Bereczky, Z.; Deak, A.; Nemeth, N. In vitro effects of temperature on red blood cell deformability and membrane stability in human and various vertebrate species. Clin Hemorheol Microcirc **2021,** 78, 291-300.
37. Suzuki, T.; Takao, H.; Suzuki, T.; Fujimura, S.; Hataoka, S.; Kodama, T.; Aoki, K.; Ishibashi, T.; Yamamoto, M.; Yamamoto, H.; Murayama, Y. Development of patient-specific apparent blood viscosity predictive models for computational fluid dynamics analysis of intracranial aneurysms with machine learning approaches. Comput. Methods Programs Biomed. **2025,** 268, 108831.
38. Riva, A.; Sturla, F.; Caimi, A.; Pica, S.; Giese, D.; Milani, P.; Palladini, G.; Lombardi, M.; Redaelli, A.; Votta, E. 4D flow evaluation of blood non-Newtonian behavior in left ventricle flow analysis. J Biomech **2021,** 119, 110308.
39. Pries, A.R.; Neuhaus, D.; Gaehtgens, P. Blood viscosity in tube flow: dependence on diameter and hematocrit. Am. J. Physiol. **1992,** 263, H1772-H1778.
40. Chien, S. Shear dependence of effective cell volume as a determinant of blood viscosity. Science **1970,** 168, 977-979.
41. Noh, S.-M. Clinical significance of blood viscosity in patients with acute ischemic stroke. Sci. Rep. **2025,** 15, 22424.
42. Mooney, M. The viscosity of a concentrated suspension of spherical particles. J. Colloid Sci. **1951,** 6, 162–170.
43. Krieger, I.M.; Dougherty, T.J. A mechanism for non-Newtonian flow in suspensions of rigid spheres. Transactions of the Society of Rheology **1959,** 3, 137-152.
44. Tao, R.; Huang, K. Reducing blood viscosity with magnetic fields. PHYS. Rev. E **2011,** 00, 001900.
45. Hund, S.; Kameneva, M.; Antaki, J. A quasi-mechanistic mathematical representation for blood viscosity. Fluids **2017,** 2, 10.
46. Bull, B.S.; Fujimoto, K.; Houwen, B.; Klee, G.; Hove, L.v.; Assendelft, O.W.v. International council for standardization in haematology (ICSH) recommendations for surrogate reference method for the packed cell volume. Lab. Hematol. **2003,** 9, 1-9.
47. Pearson, T.C.; Guthrie, D.L. Trapped plasma in the microhematocrit. Am. J. Clin. Pathol. **1982,** 78, 770–772.
48. Livshits, L.; Bilu, T.; Peretz, S.; Bogdanova, A.; Gassmann, M.; Eitam, H.; Koren, A.; Levin, C. Back to the gold standard: how precise is hematocrit detection today? Mediterr. J. Hematol. Infect. Dis. **2022,** 14, e2022049.

 doi:10.20944/preprints202603.2339.v1

49. Merlo, A.; Losserand, S.; Yaya, F.; Connes, P.; Faivre, M.; Lorthois, S.; Minetti, C.; Nader, E.; Podgorski, T.; Renoux, C.; Coupier, G.; Franceschini, E. Influence of storage and buffer composition on the mechanical behavior of flowing red blood cells. Biophys. J. **2023,** 122, 360-373.
50. Turner, T.; Hansen, A.; Kurach, J.; Acker, J.P. From development to implementation: adjusting the hematocrit of deglycerolized red cell concentrates to meet regulatory standards. Transfus. Med. Hemother. **2017,** 44, 30-38.
51. Oksuz, C.; Bicmen, C.; Tekin, H.C. Dynamic fluidic manipulation in microfluidic chips with dead-end channels through spinning: the Spinochip technology for hematocrit measurement, white blood cell counting and plasma separation. Lab Chip **2025,** 25, 1926-1937.
52. Kang, Y.J. Quantitative monitoring of dynamic blood flows using coflowing laminar streams in a sensorless approach. Applied Sciences **2021,** 11, 7260.
53. O'Brien, S.; Kent, N.J.; Lucitt, M.; Ricco, A.J.; McAtamney, C.; Kenny, D.; Meade, G. Effective hydrodynamic shaping of sample streams in a microfluidic parallel-plate flow-assay device: matching whole blood dynamic viscosity. IEEE Trans Biomed Eng **2012,** 59, 374-82.
54. Guillot, P.; Panizza, P.; Salmon, J.-B.; Joanicot, M.; Colin, A. Viscosimeter on a microfluidic chip. Langmuir **2006,** 22, 6438-6445.
55. Kim, G.; Jeong, S.; Kang, Y.J. Ultrasound standing wave-based cell-to-liquid separation for measuring viscosity and aggregation of blood sample. Sensors (Basel) **2020,** 20, 2284.
56. Pirofsky, B. The determination of blood viscosity in man by a method based on Poiseuille's law. J. Clin. Invest. **1953,** 32, 292-298.
57. Rand, P.W.; Lacombe, E. Hemodilution, tonicity, and blood viscosity. J. Clin. Invest. **1964,** 43, 2214-2226.
58. Flormann, D.; Schirra, K.; Podgorski, T.; Wagner, C. On the rheology of red blood cell suspensions with different amounts of dextran: separating the effect of aggregation and increase in viscosity of the suspending phase<2016_Flormann-2016-On-the-rheology-of-red-blood-cell-s.pdf>. Rheol. Acta **2015,** 55, 477–483.
59. Soutani, M.; Suzuki, Y.; Tateishi, N.; Maeda, N. Quantitative evaluation of flow dynamics of erythrocytes in microvessels: influence of erythrocyte aggregation. Am. J. Physiol. **1995,** 268, H1959-H1965.
60. Kang, Y.J. Microfluidic chip for quantitatively assessing hemorheological parameters. Micromachines **2025,** 16, 567.
61. Bosek, M.; Ziomkowska, B.; Pyskir, J.; Wybranowski, T.; Pyskir, M.; Cyrankiewicz, M.; Napiorkowska, M.; Durmowicz, M.; Kruszewski, S. Relationship between red blood cell aggregation and dextran molecular mass. Sci. Rep. **2022,** 12, 19751.
62. Carr, R.; Cockelet, G.R. Rheology of suspensions of normal and hardened erythrocytes and their mixtures. J. Rheol. **1981,** 25, 67-82.
63. Perazzo, A.; Peng, Z.; Young, Y.-N.; Feng, Z.; Wood, D.K.; Higgins, J.M.; Stone, H.A. The effect of rigid cells on blood viscosity: linking rheology and sickle cell anemia. Soft Matter **2022,** 18, 554-565.
64. Chien, S.; Usami, S.; Dellenback, R.J.; Gregersen, M.I. Blood viscosity: influence of erythrocyte deformation. Science **1967,** 157, 827-829.